Total Cross Section for $p + d \rightarrow p + d + \pi^0$ Close to Threshold

H. Rohdjess,[1] W. Scobel,[1] H. O. Meyer,[2] P. V. Pancella,[3] S. F. Pate,[2],[a] M. A. Pickar,[4] R. E. Pollock,[2] B. v. Przewoski,[2] T. Rinckel,[2] P. P. Singh,[2] F. Sperisen,[2] and L. Sprute[1]

[1] *I. Institut für Experimentalphysik, Universität Hamburg, Hamburg, Germany*

[2] *Department of Physics, Indiana University, and Indiana University Cyclotron Facility, Bloomington, Indiana 47405*

[3] *Western Michigan University, Kalamazoo, Michigan 49008*

[4] *Department of Physics and Astronomy, University of Kentucky, Lexington, Kentucky 40506*

(Received 16 February 1993)

The total cross section for pion production in the reaction $pd \rightarrow pd\pi^0$ has been measured for bombarding energies from $T_p = 208.4$ MeV to 294.6 MeV. This corresponds to maximum pion momenta $\eta = p_{\pi,\mathrm{c.m.}}/m_\pi c$ between 0.099 and 0.96. The experiment was performed using an electron-cooled proton beam and an internal deuterium gas jet target. The resulting σ_{tot} changes by almost 4 orders of magnitude over the covered energy range. The results are compared to a model which assumes quasi-free production via the $pn \rightarrow d\pi^0$ elementary process.

PACS numbers: 25.40.Qa, 13.75.Cs, 25.10.+s

Pion production in the three-nucleon system is of fundamental importance in a study of many-body contributions to the inelastic part of the nucleon-nucleon (NN) interaction. With three participating nucleons, effects of the nuclear environment could start to play a role, while there is still hope for a detailed theoretical treatment. In the reaction $pd \rightarrow pd\pi^0$, for instance, a single nucleon is added to the nucleon-nucleon (NN) channels $pp \rightarrow pp\pi^0$, $pn \rightarrow pn\pi^0$, and $pn \rightarrow d\pi^0$, and thus it is tempting to relate $pd \rightarrow pd\pi^0$ to the elementary processes $NN \rightarrow NN\pi^0$, with the additional nucleon being a spectator. Departure from this quasi-free mechanism due to the influence of the nuclear environment should be more easily understood than in any other exclusive (N, π) reaction, because the deuteron wave function is well explored. The situation is further simplified when the energy T_p is close to the threshold value of 207.36 MeV. Here the nonresonant amplitudes dominate, and the angular momenta accessible in the exit channel are restricted to s and p waves for the NN subsystem, and for the pion relative to the NN system [1–4].

Recently, the total cross sections for the reactions $pp \rightarrow pp\pi^0$ and $pn \rightarrow d\pi^0$ have been measured close to threshold [2,3]. They represent an excellent basis for a study of the possible role of $NN \rightarrow NN\pi^0$ production in the pd system. It is the aim of the present work to provide, for the first time, total cross sections for $pd \rightarrow pd\pi^0$ near threshold, i.e., for maximum pion momenta $p_{\pi,\mathrm{c.m.}}/m_\pi c = \eta \leq 1$. So far, there is virtually no cross-section information on $pd \rightarrow pd\pi^0$ available. Hogstrom *et al.* [5] conclude from a study of the differential cross section of $pd \rightarrow nd\pi^+$ at $T_p = 585$ MeV that at this higher energy several reaction mechanisms could contribute. Meyer [6] argues that at threshold $pn \rightarrow d\pi^0$ is expected to be the main contributor among the elementary processes.

In the present experiment the events of interest are identified by the detection of the pd pair with subsequent reconstruction of the missing π^0 mass. This has to be achieved in the presence of high rates from elastic scattering and deuteron breakup, $pd \rightarrow ppn$. The experiment has been performed at the Indiana University Cyclotron Facility Cooler Ring, where the electron-cooled proton beam, in combination with a windowless gas-jet target, provides the clean experimental environment needed for this threshold measurement [7]. The beam energy resolution of better than 60 keV makes feasible the measurement of the steep rise of $\sigma_{\mathrm{tot}}(T_p)$ above threshold. The following paragraphs outline the experimental setup.

An internal D_2 gas-jet target provides thicknesses of $(0.5\text{–}1.5)\times 10^{15}$ nuclei/cm^2. After injection, about 10^9 protons are stored. A high time-averaged luminosity of 0.5×10^{30} cm^{-2} s^{-1} is achieved with beam lifetimes on the order of 50 s. The reaction products leave the downstream end of the target chamber through a thin stainless steel exit foil. The target is mounted in one of two positions with respect to the exit foil. The angular range available for particle detection is $2° \leq \Theta_{\mathrm{lab}} \leq 11°$ (geometry 1), or $4° \leq \Theta_{\mathrm{lab}} \leq 19°$ (geometry 2). The beam pipe in the center of the detector prevents particle detection for $\Theta_{\mathrm{lab}} \leq 2°$.

The detector stack is composed of five layers perpendicular to the beam. Two segmented layers of plastic scintillators measure energy (E) and time of flight for both charged particles in coincidence. A third one allows discrimination against protons with $E_p > 120$ MeV which cannot arise from $pd \rightarrow pd\pi^0$. Two pairs of wire chambers each provide two-dimensional position information. Further details on detector components can be found in [3]. All detector layers were kept as thin as possible to accommodate the low average energy of protons from the reaction $pd \rightarrow pd\pi^0$. This way final-state proton energies as low as 17 MeV could be measured. Data were accumulated at 27 different energies T_p with integrated luminosities ranging from 3 to 26 nb^{-1} per energy setting.

Valid two-prong events have to satisfy conditions imposed on the hit pattern of the four wire planes and on the resulting vertex reconstruction. Protons and deuterons are identified by their energy and their time of flight; for proton-deuteron coincidences, the missing mass of the unobserved particle is reconstructed. Above threshold they show a clean peak at the π^0 mass at 135 MeV/c^2 (Fig. 1); a gate (G) on this peak as indicated is applied to identify $pd \rightarrow pd\pi^0$ events. The background has been estimated from a subthreshold run at $T_p = 200$ MeV; see Fig. 1.

The fraction of $pd \rightarrow pd\pi^0$ events that can be detected and reconstructed with the apparatus (i.e., the acceptance) was determined by a Monte Carlo simulation of the setup. The main reason for inefficiency is the limited angular acceptance of the detector array. The distribution of $pd \rightarrow pd\pi^0$ events in phase space establishes the size of the correction for that part of the phase space which is not covered. For the lowest participating partial waves in the pd system ($L = 0$) and for the pion with respect to the nucleons ($l = 0$) the population is uniform. The pd final state interaction (FSI) in the $L = 0$ channel gives rise to nonuniformities, and so do higher partial waves ($l, L > 0$). In the simulation, the FSI was treated following [8], using an effective range expansion with parameters taken from [9], and higher partial waves were introduced in a zero-range approximation [10]. At energies with $\eta \geq 0.3$, FSI and higher partial waves, especially contributions with $L = 1$ and $l = 0$, are needed to reproduce the experimental distributions in angle and energy of the outgoing protons and deuterons. Figure 2 shows that the main loss of acceptance for $pd \rightarrow pd\pi^0$ events is due to protons emitted at angles larger than the maximum detection angle. This limit is reached for $T_p > 209$ MeV (in geometry 2: 214 MeV), whereas for the deuterons this constraint is uncritical.

A systematic uncertainty of (5–35)% for the calculated acceptance was obtained by varying the assumptions in the simulation while still reproducing the measured angle and energy distributions [11]. The large uncertainties arise at the higher energies, where the relative importance of different partial waves cannot be determined unambiguously. Other corrections include wire-chamber (2%) and scintillator (< 5%) inefficiencies, and the losses in the material between the target and E detector, i.e., nuclear proton absorption and deuteron breakup (<1%) and protons with energies low enough to be stopped (<10%). The resulting, energy dependent acceptance for both geometries is shown in Fig. 2.

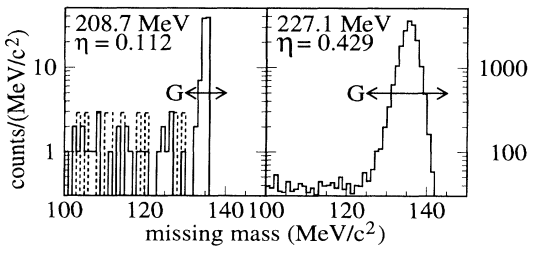

FIG. 1. Distribution of the reconstructed missing masses; the dashed histogram on the left represents a subthreshold run ($T_p = 200$ MeV) normalized to the same luminosity.

The simulation also showed that the response of the detector to channels like $pd \rightarrow ppn$ or $\rightarrow ppn\pi^0$ is negligible when the $pd \rightarrow pd\pi^0$ conditions are applied. The projectile energy was determined from the frequency of the beam bunching rf cavity and the circumference of the ring (86.82 ± 0.03 m). The absolute calibration was obtained to a precision of ±200 keV as in [3] by comparing the strongly energy dependent maximum laboratory angle of the protons and deuterons with the simulation.

The absolute normalization of the cross section is derived from a simultaneous measurement of $p + d$ elastic scattering. Four position-sensitive silicon detectors (PSD), two on either side of the gas jet, measure energy and position of the recoil deuteron in coincidence with the forward proton. The position information is used to reconstruct the vertex distribution along the beam axis. It is extrapolated beyond the limits of the PSD acceptance to obtain contributions to the luminosity of the uniform gas density [(20–30)%] within the inner differential pumping stage surrounding the jet target. The (previously unknown) $p + d$ elastic differential cross section for projectile energies in the range 200–294 MeV has been deduced from the (known) $p + p$ elastic cross section ([12], solution VZ40) by a concurrent measurement of $p + p$ and $p + d$ elastic scattering rates [13]. This measurement was performed with HD gas as a target. The luminosities obtained give rise to an energy dependent absolute normalization error of the $pd \rightarrow pd\pi^0$ cross section ranging from 5% to 8%, which is almost entirely due

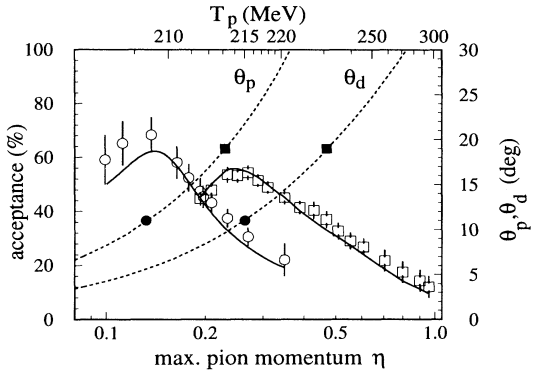

FIG. 2. Detector acceptance vs η for geometry 1 (circles) and 2 (squares). The solid lines result from a pure phase space distribution, and the indicated open symbols include corrections from FSI and higher partial waves. The lines labeled Θ_p (Θ_d) show the maximum laboratory angles for reaction protons (deuterons), and the solid symbols the detector limitation in angle.

to uncertainties in the $p+p$ elastic cross section.

The final $pd \rightarrow pd\pi^0$ cross sections obtained during this experiment are listed in Table I and plotted versus η as triangles in Fig. 3. The observed consistency between data obtained with the two different geometries (up and down triangles) is strong evidence for the validity of the correction for detector acceptance. The error bars include statistical and systematic contributions and the uncertainty of the beam energy. Usually, the uncertainties are smaller than the size of the symbols.

Also shown are total cross sections for the reactions $pn \rightarrow d\pi^0$ [2] (squares, the dotted line represents a fit to all available data) and $pd \rightarrow {}^3\mathrm{He}\,\pi^0$ [4] (circles) for the same range of maximum pion momenta. One can see that the measured $pd \rightarrow pd\pi^0$ cross section is much smaller than the corresponding $pn \rightarrow d\pi^0$ cross section (at the lowest energy by 3 orders of magnitude). It is remarkable that the addition of a spectator proton (to go from $pn \rightarrow d\pi^0$ to $pd \rightarrow pd\pi^0$) should have such a large effect on the pion production cross section. It can be shown, however, that the suppression of the $pn \rightarrow d\pi^0$ cross section, when embedded in the three nucleon system, is understood quite easily [6]: At threshold, all reaction products are at rest in the center-of-mass system. This fixes their momentum in the laboratory system. The spectator proton, true to its nature, must have had the same momentum *before* the interaction when it was part of the target deuteron. The neutron in the target deuteron (which rests in the laboratory) thus must have opposite momentum k_n, which is directed towards the projectile with a magnitude of about 200 MeV/c (or 1 fm^{-1}), where the momentum density in the deuteron is about 10^3 times lower than at $k_n = 0$. The dashed line in Fig. 3 indicates the $pd \rightarrow pd\pi^0$ cross section which would follow from the assumption that the *only* contributing process is quasi-free production via the $pn \rightarrow d\pi^0$ channel. The details of this calculation will be published in a separate paper [14]. The importance of this mechanism for the subthreshold pion production, in the case $^{12}\mathrm{C}(p, d\pi^+)^{11}\mathrm{B}$, has been indicated in [15].

TABLE I. Experimental values of $pd \rightarrow pd\pi^0$ total cross sections, and related quantities.

T_p (MeV)	η (10^{-3})	Number of events	σ_{tot}	Geometry
208.4	99 ± 9	62	5.5 ± 1.2 nb	1
208.7	112 ± 8	86	7.1 ± 1.3 nb	1
209.4	137 ± 7	219	18.8 ± 2.5 nb	1
210.3	164 ± 6	364	41.8 ± 5.5 nb	1
210.8	178 ± 5	430	61.9 ± 7.8 nb	1
211.4	193 ± 5	674	84.8 ± 10.8 nb	1
211.4	193 ± 5	335	83.3 ± 8.5 nb	2
211.6	197 ± 5	701	92.9 ± 10.7 nb	1
212.1	209 ± 4	574	119 ± 14 nb	1
212.1	209 ± 4	567	101 ± 9 nb	2
213.3	234 ± 4	873	184 ± 21 nb	1
213.3	234 ± 4	623	158 ± 15 nb	2
214.2	251 ± 4	494	208 ± 19 nb	2
215.3	270 ± 3	566	318 ± 42 nb	1
215.3	270 ± 3	754	290 ± 25 nb	2
216.5	290 ± 3	1275	369 ± 30 nb	2
217.8	311 ± 3	1650	522 ± 42 nb	2
220.6	349 ± 3	465	614 ± 175 nb	1
220.6	349 ± 3	1751	846 ± 74 nb	2
223.7	389 ± 2	3472	1.27 ± 0.11 μb	2
227.1	429 ± 2	17 739	1.81 ± 0.18 μb	2
230.7	469 ± 2	4490	2.57 ± 0.27 μb	2
234.7	509 ± 2	6554	3.65 ± 0.41 μb	2
239.4	554 ± 2	5691	5.64 ± 0.72 μb	2
245.4	607 ± 2	7756	7.74 ± 1.04 μb	2
257.4	704 ± 2	14 721	13.7 ± 2.7 μb	2
270.5	799 ± 1	10 056	22.5 ± 5.4 μb	2
285.5	901 ± 1	18 916	35.5 ± 10.3 μb	2
294.6	959 ± 1	43 893	44.6 ± 14.7 μb	2

It is expected that the "nuclear medium," in this case the spectator, affects the quasi-free process. One can consider the FSI between the outgoing pd pair to be the first order approximation to this effect. Including the FSI in the quasi-free calculation, in the manner described earlier in this paper, results in the solid curve in Fig. 3 (for details, see [14]). In this calculation the absolute value is not fixed (as it is for the dashed line), but already the close agreement in the energy dependence of the reaction is strong evidence for the importance of the FSI. The prominent role of the bound state of the $p+d$ system in the exit channel is also illustrated by the magnitude of the $pd \rightarrow {}^3\mathrm{He}\,\pi^0$ cross section (circles in Fig. 3). A study of additional medium effects would have to be based on more detailed experimental information on angular and energy distributions.

In conclusion, we have measured the $pd \rightarrow pd\pi^0$ total cross section close to threshold. A quasi-free reaction model containing the dynamics of the deuteron provides a fair description of the data. This supports the idea that

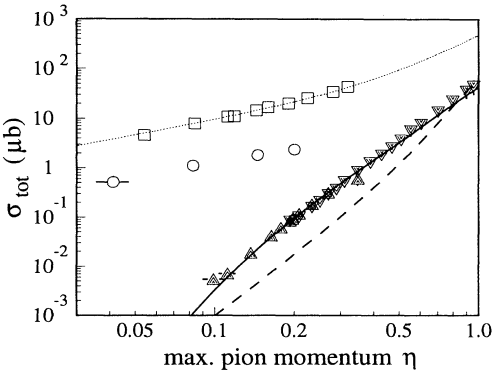

FIG. 3. Total cross sections vs η for the reactions $pd \rightarrow pd\pi^0$ (triangles, this work), $np \rightarrow d\pi^0$ (squares, [2]), and $pd \rightarrow {}^3\mathrm{He}\pi^0$ (circles, [4]). The lines are explained in the text.

pion production in nuclei is dominated by short-range $NN \rightarrow NN\pi^0$ interactions, filtered by the properties of the nucleus and by the requirements of the kinematics of the reaction.

This work has been supported by the German BMFT under Contract No. 06HH613, by the U.S. NSF under Grants No. PHY 90-15957 and No. PHY-9103794, and by the FRACASF (Western Michigan University). We thank the operating team of the IUCF Cooler for the excellent beam support and gratefully acknowledge the work of J. Doskow in installing and testing the gas-jet target.

[a] Present address: Laboratory for Nuclear Science, MIT Cambridge, MA 02139.

[1] A. H. Rosenfeld, Phys. Rev. **96**, 139 (1954).
[2] D. H. Hutcheon *et al.*, Phys. Rev. Lett. **64**, 176 (1990).
[3] H. O. Meyer *et al.*, Nucl. Phys. **A539**, 633 (1992).
[4] M. A. Pickar *et al.*, Phys. Rev. C **46**, 397 (1992).
[5] K. R. Hogstrom *et al.*, Phys. Rev. C **17**, 259 (1978).
[6] H. O. Meyer (to be published).
[7] R. E. Pollock, Annu. Rev. Nucl. Sci. **41**, 357 (1991).
[8] K. M. Watson, Phys. Rev. **88**, 1163 (1952).
[9] J. Arvieux, Nucl. Phys. **A221**, 253 (1974).
[10] K. M. Watson and K. A. Brueckner, Phys. Rev. **83**, 1 (1951).
[11] H. Rohdjess, Ph.D. thesis, Universität Hamburg, 1993 (unpublished).
[12] R. A. Arndt *et al.*, Phys. Rev. D **28**, 97 (1983); R. A. Arndt, interactive program SAID.
[13] H. Rohdjess *et al.* (to be published).
[14] H. O. Meyer and J. A. Niskanen, Phys. Rev. C (to be published).
[15] A. A. Cowley *et al.*, Phys. Rev. C **45**, 1745 (1992).